Compact Hollow Waveguide Mid-Infrared Gas Sensor For Simultaneous Measurements of Ambient CO 2 and Water Vapor

Tao Wu, Weiping Kong, Mengyu Wang, Qiang Wu, Weidong Chen, Chenwen Ye, Rongjing Hu, Xingdao He

Compact hollow waveguide mid-infrared gas sensor for simultaneous measurements of ambient CO_2 and water vapor

Tao Wu, Weiping Kong, Mengyu Wang, Qiang Wu, Weidong Chen, Chenwen Ye, Rongjing Hu, Xingdao He

***Abstract*—A compact, sensitive and stable hollow waveguide (HWG) mid-infrared gas sensor, based on gas absorption lines using wavelength modulation spectroscopy with a second harmonic (WMS-2*f*) detection scheme, was developed for simultaneous measurements of ambient CO_2 and water vapor. Optimization of the laser modulation parameters and pressure parameter in the HWG are performed to improve the strength of the WMS-2f signal and hence the detection limit, where 14.5-time for CO_2 and 8.5-time for water vapor improvement in system detection limit is achieved compared to those working at 1atm. The stability of the sensor has been improved significantly by optimizing environmental disturbances, incoupling alignment of the HWG and laser scanning frequency. An Allan variance analysis shows detection limit of the developed sensor of ~ 3 ppmv for CO_2 and 0.018 % for water vapor, which correspond to an absorbance of 2.4×10^{-5} and 2.7×10^{-5}, with a stability time of 160 s, respectively. Ambient CO_2 and water vapor measurement have been performed in two days in winter and spring separately. The measurement precision is further improved by applying a Kalman adaptive filter. The HWG gas sensor demonstrates the ability in environmental monitoring and the potential to be used in other areas, such as industrial production and biomedical diagnosis.**

***Index Terms*—Hollow waveguide, wavelength modulation absorption spectroscopy, carbon dioxide, water vapor.**

I. Introduction

Carbon dioxide (CO_2) and water vapor (H_2O) are important atmospheric species, which both regulate the global temperature change [1] and the growth of the biospheric vegetation. Measurements of the changes in concentration of CO_2 and H_2O across the time and space scales play an important role in the modeling of the carbon cycle and the water cycle in the atmosphere [2,3]. Among numerous trace gas detection techniques, technique based on laser absorption spectroscopy [4] is well established for trace gas detection due to its long-term stability, portability, high sensitivity and selectivity. In order to improve the measurement sensitivity of laser absorption spectroscopy technique, folding the optical path within the sample cell is usually used, including White cell [5], Herriott cell [6] and high finesse optical cavity [7]. However, these cells have a large volume (>100ml) [8], a high cost and a large physical size. Especially, large volume will lead to a low sampling rate and a high sampling gases and standard gases consumption, which limits its application in the situation of requiring simultaneously high sampling rate and high sample refreshing rate, as well as measurement a small amount of gas sample (e.g. <10 ml).

The HWG was first proposed by Garmire et al. [9] in 1976. It has been continuously evolved and spread to numerous applications [10-17], and is generally defined as a capillary tube whose core is air and surrounding has a refractive index higher than 1.0. In order to reduce the light propagation loss, the HWG is usually coated with a metallic layer of Ag on the inner wall of the silica glass tubing [18] and then a dielectric layer of AgI over the metal film [19]. The transmission range of the HWG is usually from 2.6 to 10.6 μm, which is the wavelength region of interest by a lot of applications in trace gas detection. The hollow waveguide (HWG), serving as light guides and gas transmission cell simultaneously, are an elegant alternative to address both requirements, hence has been regarded as a valuable gas absorption cell for TDLAS based measurements. Compared with traditional folded gas cell, a HWG cell has a low internal volume (several milliliters) and the extended optical path (several meters) with low cost [15], which causes faster response times (several seconds) [16] and high sensitivity. Furthermore, the HWG can be coiled into relatively small spaces to save gas cell space [20]. Due to the light weight and compact size of the HWG itself, the use of HWG as the gas cell of the spectroscopic system can effectively reduce the weight and size of the entire measurement system. These advantages make the HWG applied in compact, low-cost, sensitive, and accurate sensor suitable for environmental monitoring, industrial production and biomedical diagnosis.

Manuscript received December 24, 2019. This work was supported in part by the Key Research and Development Program of Jiangxi Province, China, under Grant 20192BBH80019. (Corresponding authors: Tao Wu; Qiang Wu.)

T. Wu, W. Kong, M. Wang, C. Ye, R. Hu and X. He are with the Key Laboratory of Nondestructive Test (Ministry of Education), Nanchang Hangkong University, Nanchang 330063, China (e-mail: wutccnu@nchu.edu.cn; 1090049692@qq.com; mengyu@nchu.edu.cn; 23022@nchu.edu.cn; mayhrj@nchu.edu.cn; hxd@nchu.edu.cn).

Q. Wu is with the Department of Physics and Electrical Engineering, Northumbria University, Newcastle upon Tyne NE1 8ST, U.K. (e-mail: qiang.wu@northumbria.ac.uk).

W. Chen is with the Laboratoire de Physicochimie de l'Atmosphère, Université du Littoral Côte d'Opale, 59140 Dunkerque, France (e-mail: chen@univ-littoral.fr).

However, the small physical size of the HWG renders it susceptible to unwanted mechanical vibrations and temperature fluctuations. Further, many fiber mode-dependent physical effects may result in fiber noise. These reasons all lead to instability of the HWG sensor, especially for long term operation. In order to solve this problem, Fetzer et al [21] mounted the HWG with a steel chassis to reduce its mechanical vibration and used a 5 degrees of freedom mechanical device to mode-match the laser beam to the input of the waveguide to reduce the system signal drift. In order to reduce background noise, Chen et al [22] added a 200 Hz vibration to the HWG fiber and optimized the vibration amplitude to achieve an optimal sensor baseline, which hence increased the sensor sensitivity. So far, only a few studies [21-22] have investigated the system drift uncompensated by intensity fluctuations of the HWG based sensor, and no real-time measurements of atmospheric gases by the HWG based sensor has been reported.

In the present work, a stable and sensitive HWG gas sensor was developed for simultaneous measurement of atmospheric CO_2 and water vapor absorption. The laser modulation parameters (modulation amplitude, modulation frequency, reference phase, time constant of lock-in amplifier) and the gas pressure in the HWG were optimized to achieve the maximum strength of the WMS-2f signal. Environmental disturbing (mechanical vibrations and temperature fluctuations), the influence of incoupling and outcoupling alignment of the HWG sensor, and the effect of laser scanning frequency are taken into account to improve the stability of the HWG sensor. The detection limit and system stabilization time of HWG gas sensor are comparable with those previously reported values. Finally, the hollow waveguide gas sensor was used to measure atmospheric CO_2 and water vapor simultaneously in the real-time and the measurement precision was improved greatly by applying a Kalman adaptive filter.

II. Experimental Section

A. Selection of absorption lines

Measurements of ambient CO_2 and water vapor require simultaneously probing of the absorption lines of CO_2 and H_2O within laser wavelength scanning range. It is demanded that the selected absorption lines are free from interference from other species and possess large absorption intensity at the same time.

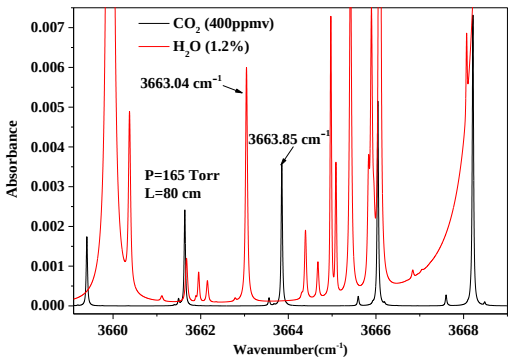

Fig. 1 Absorption spectra of 400 ppmv CO_2 and 1.2 % H_2O at a pressure of 165 torr with a light path length of 80 centimeter.

Figure 1 depicts the absorption spectral simulation of CO_2 and H_2O at typical ambient mixing ratios (400 ppmv CO_2 and 1.2 % H_2O) at a pressure of 165 torr near 2.73 μm using the data from the HITRAN database [23]. The absorption peak of CO_2 at 3663.85 cm^{-1} and the absorption peak of water vapor at 3663.04 cm^{-1} were selected.

B. Experimental set-up

1) Optical platform and waveguide coupling system

A three-dimensional (3D) view of the HWG-based gas sensor is shown in Fig. 2. The optical head of the sensor (including laser, detector, mirrors and mounts) is fixed on the optical breadboard with a physical size of 45×30×12 cm^3, power supplies and controllers are housed around the optical head. A 2.73 μm DFB laser diode (Nanoplus GmbH, Germany) with a spectral tuning range from 3658cm^{-1} to 3670cm^{-1} and a maximum output power of 11.2 mW is used to probe CO_2 and H_2O vapor absorption lines. The DFB laser is packaged in a TO5 cube, assembled with a thermoelectric cooler (TEC), and equipped with a collimating lens. The laser beam is coupled into the HWG gas sensor with two mirrors. To reduce the interference resulting from indoor air, the distance between laser and HWG gas cell is shortened as possible. The custom-made HWG gas cell is formed by a HWG (Polymicro, HWEAC10001600, USA) with an effective length of 80 cm and two customized mounts, which are connected together by silicon glue. A Calcium Fluoride (CaF_2) wedged window is sealed on the mount via an O-ring to prevent leakage of the gas from the HWG. The volume of the custom-made HWG gas cell is 0.78 cm^3. Light beam exiting the HWG is detected by a thermoelectrically cooled HgCdTe photovoltaic detector (VIGO system, PVI-4TE-10.6, Poland).

2) Laser control and data acquisition system

Laser diode is operated with a laser controller (ILX Lightwave, LDC-3724C, USA). A sine wave (4 kHz) provided by a lock-in amplifier (Stanford Research System, SR830, USA) and a sawtooth wave (30 Hz) generated by a function generator are summed by an analog adder as laser drive signal sent to the current modulation port of the laser controller. The signal output of the detector is delivered to lock-in amplifier for obtain the WMS-2f signals. The in-phase signal of the lock-in amplifier is acquired by a data acquisition card (ADlink, DAQ-2010, China) and stored by a Labwindows program installed in a computer. The data acquisition card is triggered by the function generator to synchronize the entire signal processing system.

3) Gas delivery system

As shown in Fig. 2, the CO_2 samples with different concentrations are prepared by a dynamic dilution of a 4000 ppmv CO_2 standard mixture to pure nitrogen. A variety of CO_2 concentrations are produced by adjusting the flow rates of two MFCs (MKS Instruments GV50A, USA). The water vapor concentration is calibrated using a dew point generator (DPG, LI-COR, LI-610, USA). A tee-split (‘Bypass’ in Fig. 2) was used in the outlet of DPG to avoid over-pressurization of the DPG. The ambient air is sampled through a 4-meter long PFA

tube with a PTFE filter, and a cut-off valve is used to control the on and off of the sampling. The pressure in the HWG gas cell is controlled by a pressure controller (MKS Instruments, 640B, USA), the third MFC (MKS Instruments GV50A, USA) and a diaphragm pump.

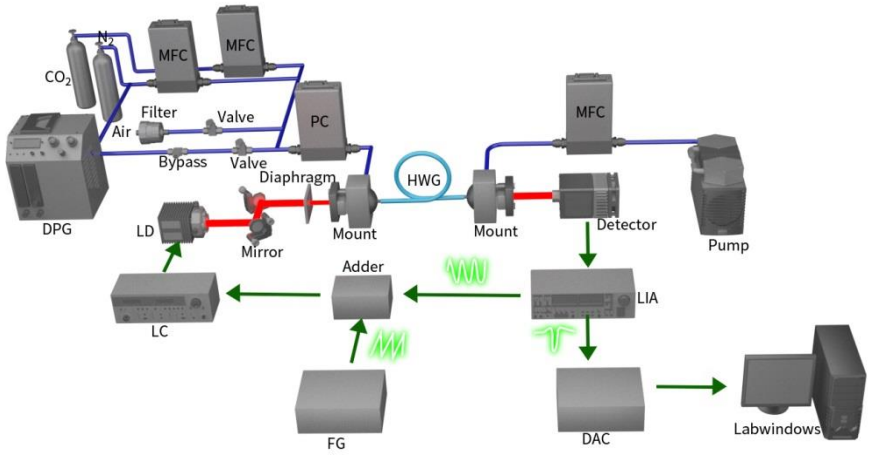

Fig. 2 3D view of the developed HWG-based gas sensor for carbon dioxide and water vapor detection. The sensor consists of three sections, including optical configuration (red line, left-to-right), laser control and data acquisition system (green arrow), and flow handling system (blue line, left-to-right). DPG: dew point generator, MFC: mass flow controller, LD: laser diode, LC: laser controller, FG: function generator, PC: pressure controller, LIA: lock-in amplifier, DAC: data acquisition card.

C. Optimization of system parameters

According to the WMS principle, the values of the 2f signal are related to modulation parameters (amplitude, frequency and phase) of the laser and the gas pressure inside the HWG. In the experiment, diluted sample gases for CO_2 with a mixing ratio of 4000 ppmv and water vapor with a concentration of 2.3% are filled into the HWG gas cell, respectively. To initially optimize the modulation parameters, we increased the modulation amplitude from 0.02 V to 0.36 V with a step of 0.02 V. In addition, we also controlled the pressure value from 100 Torr to 400 Torr. The 2f peak height with different modulation amplitudes and pressure values for both CO_2 and water vapor are shown in Fig. 3. There are two opposing effects of increasing pressure on the 2f absorption signal amplitude: decreasing absorption peak intensity due to pressure-induced spectral line broadening and improving absorber number density. In our case, at pressure range of 100-300 Torr (Lorentzian regime) the 2f signal intensity become almost constant due to the canceling of two opposing terms with pressure, while at high pressure (>300 Torr), the 2f signal amplitude decreases with pressure.

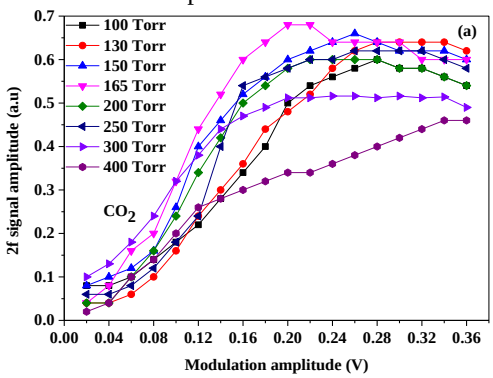

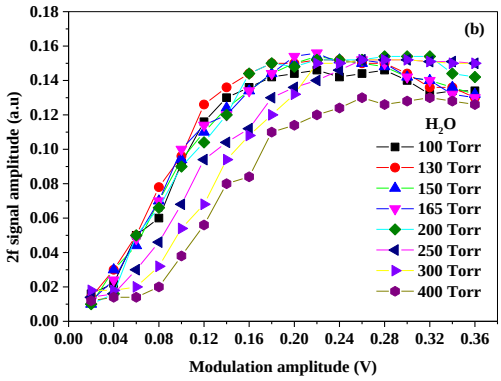

Fig. 3 Relationship between the 2f signal amplitude versus modulation amplitude for CO_2 (a) and water vapor (b).

As depicted in Fig.3 (a) and Fig.3 (b), for CO_2 and H_2O, it is obvious that the maximum value of 2f signal peak located at the point where the modulation amplitude was 0.22 V and the pressure value was 165 Torr. It is worth stressing that modulation frequency and reference phase are also optimized. The optimal modulation frequency and reference phase are 4kHz and 20 °respectively.

Most of the current spectrum measurement systems are using HWG as the gas cell working at standard atmospheric pressure [5, 9, 11, 22]. Investigation of the HWG gas sensor detection sensitivity at a pressure of 165 Torr and 760 Torr was carried out, 4000 ppmv CO_2 standard gas and 2.3% water vapor was respectively sent to the HWG gas sensor. The pressure in the HWG cell is set for 165 Torr and 760 Torr respectively and the 2f signals were recorded with an averaging time of 28 s. As shown in Fig.4 (a), the standard deviations of the 2f signals for a CO_2 standard gas at pressure of 165 Torr and 760 Torr are 1.15×10^{-3} and 1.58×10^{-3}, which leads to signal to noise ratios of about 547.6 and 37.8, respectively, thus the corresponding minimum detectable concentrations are 7.3 ppmv and 105.8 ppmv. Therefore, the HWG gas sensor for CO_2 at 165 Torr has a

14.5-time improvement compared to a pressure of 760 Torr. The standard deviations of 2f signals for water vapor at a pressure of 165 Torr and 760 Torr are 0.74×10^{-3} and 1.14×10^{-3} shown in Fig.4 (b), which leads to SNR of about 183.8 and 20.9, respectively, the corresponding minimum detectable concentrations are 0.013% and 0.11%. Therefore, the HWG gas sensor for water vapor at 165 Torr has 8.5-time improvement, as compared to the working of 760 Torr.

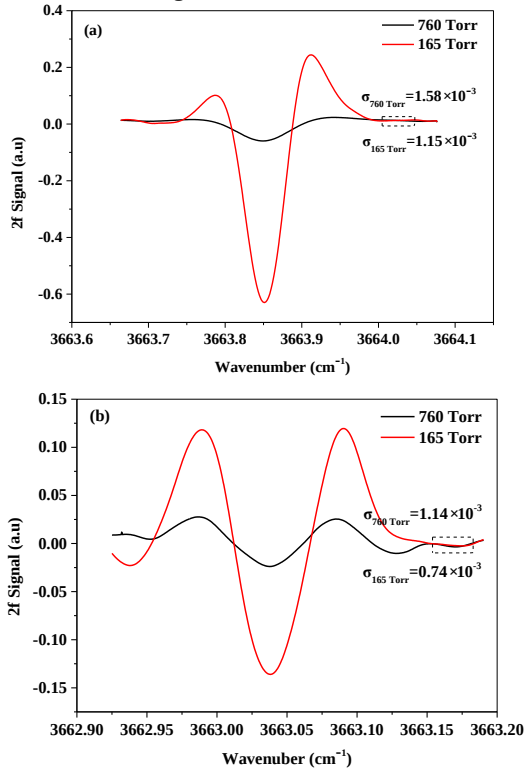

Fig. 4 The 2f signal of the HWG gas sensor at the pressure of 165 Torr and 760 Torr at the same CO_2 (a) and water vapor (b) concentration.

Mechanical vibrations and temperature fluctuations may cause drift of the HWG sensor. In order to reduce mechanical vibration induced instability to the system, the HWG is fixed on the test optical bench by tape, which has a suspension system to eliminate vibrations induced by the surrounding environment. The HWG sensor with all components is packaged in a housing, which is temperature stabilized in order to reduce ambient temperature effect. The coupling style between the laser and the HWG is available by using a focusing lens or in a direct coupling configuration. Because an additional focusing lens may produce possible optical interference by parallel optical surfaces and make the HWG sensor more complicated, direct coupling configuration is employed here. The laser beam is coupled into the HWG gas sensor with two mirrors which possess a 4 degrees of freedom mechanical device adjusting the collimating laser coupled into the center of the HWG with a small acceptance angle to reduce the number of excited modes and corresponding fiber model noise. An aperture diaphragm is placed between the laser and the HWG to modulate the laser spot size. The stability of the system for the directing coupling mode was investigated. CO_2 sample with concentration of 2000 ppmv was continuously supplied to the HWG cell, while gas pressure in the HWG cell was adjusted at a value of 165 Torr. Specifically, the aperture size of the diaphragm was successively set to 0.7 mm, 1 mm, 1.5 mm, 2 mm, 2.3 mm. Figure 5 shows the Allan variance for WMS-2*f* signals obtained with different aperture sizes of the aperture diaphragm. It is obvious that decreasing of the laser spot diameter results in increasing of the system stability time and reducing the Allan variance values, which is corresponding to available measurement sensitivity. However, the smaller aperture results in a smaller SNR, which is not conducive to improve the detection sensitivity. Hence, the aperture of diaphragm is set to 1 mm. Apart from that, the influences of in-coupling (position of the laser related to the HWG) and out-coupling (position of the detector related to the HWG) on system stability are also investigated [24]. The laser was placed at the central position for long stability time. The distance between the output of HWG and the detector was also optimized by the Allan variance analysis for WMS-2f signals.

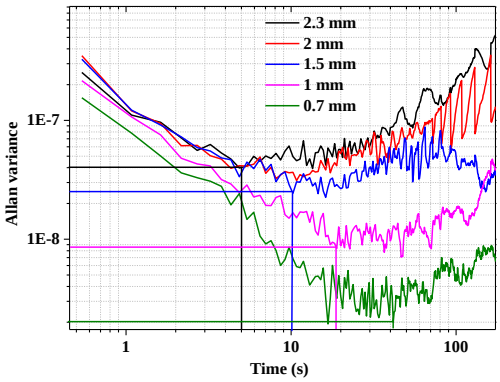

Fig. 5 The Allan variance for WMS-2*f* signals obtained with different aperture sizes of the aperture diaphragm.

The laser scanning frequency is found to affect the stability of the HWG sensor. In order to investigate its impact on the 2f signal drift, the scanning frequency was increased from 10 Hz to 50 Hz by an incremental margin of 10 Hz each time and the concentration of CO_2 in the HWG gas cell remains at 769.2 ppmv. As shown in Fig. 6, the 2f signal amplitude fluctuation with time for different scanning frequencies was obtained during 20 minutes successive measurements with 2 s intervals.

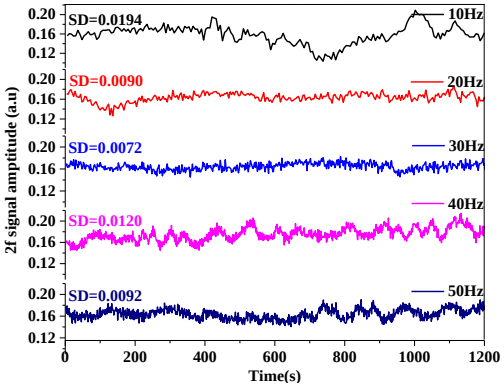

Fig. 6 2f signal amplitude fluctuations with time for different scanning frequencies.

Though a faster scan allows for the averaging of more spectra in the same acquisition time, periodic fluctuation for WMS-2*f* peak with the ramp frequency higher than 30Hz was observed. The scanning frequency of 30 Hz is best for small drift with a standard deviation (SD) of 0.0072.

D. Calibration

We controlled the pressure inside the HWG gas cell to be 165 Torr. The flow rate of the MFC2 was adjusted by a proportional value from 0-124 ml/min with a total flow rate of 130 ml/min and thus the CO_2 concentration ranges from 0 to 3815.3 ppmv. The spectra were recorded 10 times at each concentration with an average measurement time of 2 s. It is noted that although the theoretical acquisition time is 0.03 s for one spectrum, the actual measurement time is as long as 0.2 s which includes the acquisition time, data processing time and storage time. The change of water vapor concentration is realized by adjusting the operating temperature of the dew point generator. Water vapor flow is filled into the HWG gas cell by MFC3. The dew point temperature was set from 2 ℃ to 16 ℃, which causes a water vapor concentration ranging from 0.7% to 1.8%. The calibration of the CO_2 and water vapor samples was performed independently. The background signals of the CO_2 and water vapor samples were measured with pure nitrogen flowing through the cell. A plot of the background subtracted 2f signal intensity versus different concentrations of CO_2 and water vapor was respectively shown in Fig. 7 (a) and Fig. 8 (a). The 2f signal amplitudes of 10 recorded spectra at each concentration were averaged and the results are respectively plotted in Fig. 7 (b) and Fig. 8 (b) for CO_2 and water vapor. There are excellent linear relationships between the measured amplitudes of 2f signals and the CO_2/water vapor concentrations, which are used for CO_2 and water vapor measurement calibrations.

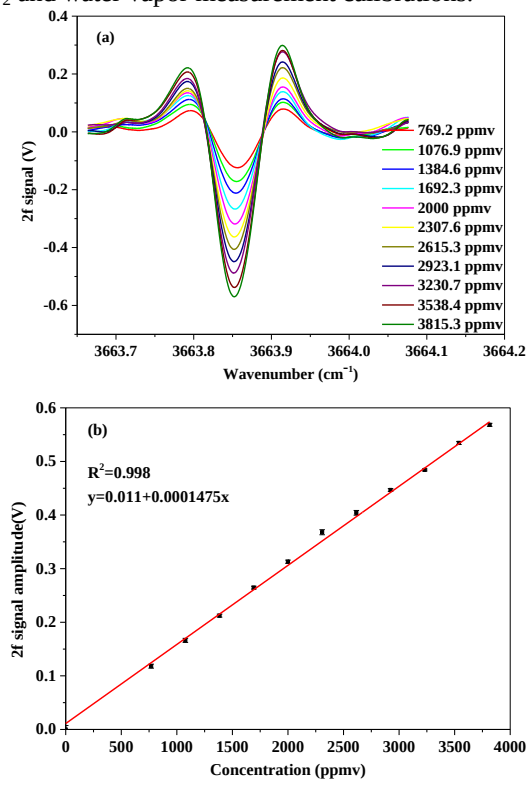

Fig. 7 (a) The background subtracted 2f signal intensity versus the different concentrations of CO_2, (b) The linear calibration functions of the HWG gas sensor.

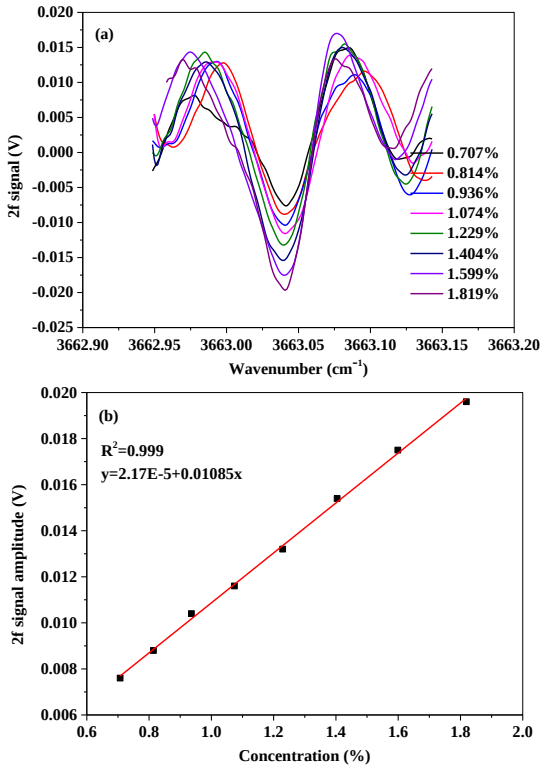

Fig. 8 (a) The background subtracted 2f signal intensity versus the different concentrations of water vapor, (b) The linear calibration functions of the HWG gas sensor for water vapor.

III. Sensor Performance

The system stability and noise feature of the HWG gas sensor have been analyzed by Allan variance [25] (as shown in Fig. 9), based on a long time-series respective measurement of CO_2 and water vapor data with constant concentrations of 1200ppmv for CO_2 and 1.6% for H_2O. The results show that the detection sensitivity of the HWG gas sensor for CO_2 and water vapor are about 26.9 ppmv and 0.14 % respectively at an average time of 1s. The detection limit of 3.0 ppmv and 0.018 % can be achieved with a stability time τ of 160s, corresponding to an absorbance of 2.4×10^{-5} and 2.7×10^{-5}. The decreasing red line $\tau^{-1/2}$ represents the theoretically expected behavior of the system dominated by white noise. When the average time is smaller than τ_{opt}, the Allan variance will decrease as the average time increases, following the red line $\tau^{-1/2}$. Table 1 shows the minimum detectable absorbance and related sytem parameters of reported HWG gas sensor. Direct absorption spectroscopy (DAS) has been used widely for absolute measurement by integrating the spectral absorbance without calibration. However, the WMS-2f enable effectively suppresses the $1/f$ noise by using a higher modulation frequency (~kHz) and hence minimum detectable absorbance using WMS is usually lower than that using DAS. Wavelength Modulation Spectroscopy with second harmonic normalized by the first harmonic (WMS-2f/1f) avoids the effect of laser intensity variation. Compared to the minimum detectable absorbance (order of 10^{-5})

and system stabilization time (160s), the developed HWG gas sensor can achieve a relatively good performance in terms of stability and sensitivity and is ideal for atmospheric gas detection. Detection limit of the HWG based sensor may be improved significantly by increasing the length of optical path via increasing length of the HWG or placing two dielectric mirrors with modest reflectivity at the two ends of the HWG to build a multi pass cavity.

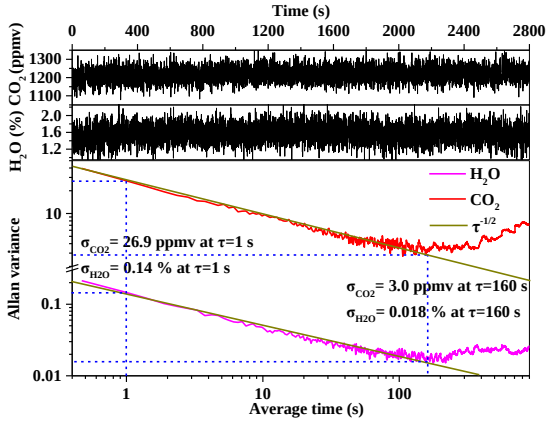

Fig. 9 The Allan variance plot of CO_2 (red line) and water vapor (pink line). The $\tau^{-1/2}$ (black line) indicates that the Allan variance is only affected by white noise.

TABLE I
Detection limit and reported system parameters of HWG gas sensor

Reference	Wavelength	Method	Optical length	Stabilization time	Absorbance
[5]	3.37 μm	WMS 2f/1f	5 m	125 s	1.1×10^{-5} (CH_3SCH_3)
[9]	7.82 μm	DAS	5 m	300 s	6.3×10^{-5} (CH_4)
[11]	3.26 μm	WMS 2f	3.3 m	24 s	5×10^{-5} (C_2H_4)
[14]	3337 nm	WMS 2f	5 m	164 s	7.4×10^{-6} (CH_3SCH_3)
[15]	3392 nm	WMS 2f	5 m	295 s	3.6×10^{-5} (CH_3SH)
[16]	3392 nm	WMS 2f/1f	75 cm	9 s	5.2×10^{-6} (CH_4)
[17]	2003 nm	DAS	12 cm	3 s	1.2×10^{-5} (CO_2)
[18]	3393 nm	DAS	5 m	1.84 s	1.34×10^{-5}(CH_3SH)
[22]	2.3 μm	WMS 2f	3 m	100 s	order of 10^{-5} (CO)
Our present work	2.73 μm	WMS 2f	80 cm	160 s	2.4×10^{-5} (CO_2) 2.7×10^{-5} (H_2O)

To evaluate the response time of the HWG gas sensor, the dynamic measurements of about 30 minutes with an average time of 1 s for different diluted CO_2 concentrations are shown in Fig. 10. The time interval between each CO_2 concentration value applied to the HWG gas sensor is about 4 mins, in which the total flow rate is set to be 130 ml/min and the CO_2 concentrations range from 0 to 3150 ppmv. The 10-90 % response time t_r and the 0-10 % delay time t_d of the HWG gas sensor those are shown in the inserts in Fig. 10. The response time t_r in rising and falling process are about 12 s and 9 s, respectively, while the delay time t_d is around 3 s.

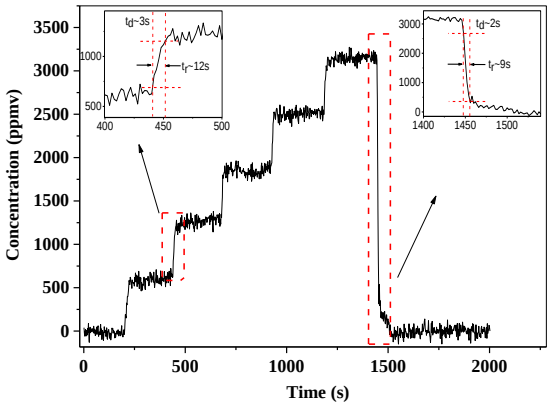

Fig. 10 Response time of the HWG gas sensor.

IV. Real-time Atmosphere Measurements

Successive measurements of ambient CO_2 and water vapor were made at Nanchang Hangkong University. The HWG gas sensor was deployed in laboratory. The ambient air was filtered by a PTFE filter and then sampled through a 4-meter long PFA tube. Experiments covered two seasons: the winter of 2018 (black points) and the spring of 2019 (blue points). Each measurement time was 5.5 hours with an interval of 1 s, as shown in Fig. 11. To further improve the detection sensitivity and the measurement precision, Kalman filtering [26] was applied in this work. Kalman filtering is an adaptive filtering technique which uses a recursive procedure for "true value" $\hat{\delta}_k$ prediction based on the previously determined "true value" $\hat{\delta}_{k-1}$ and the measured value z_k, as expressed by the following equation:

$$\hat{\delta}_k = \hat{\delta}_{k-1} + K_k\left(z_k - \hat{\delta}_{k-1}\right) \quad (1)$$

K_k is the Kalman gain, which is related to the measurement noise (σ^2_v) and the true concentration variability (σ^2_w). The filter tuning parameter ρ is defined as σ_v^2/σ_w^2. With a smaller ρ, the filtering is less efficient in removing the shot-to-shot real-time noise; conversely, when ρ is too large, the filtered result will lag behind the true variation in concentration [27].

In this work, σ^2_v was determined by the standard deviation of the first 10 measurements. The value of ρ was set from 10 to 3000. Considering the improved precision and appropriate time response, the ρ value of 600 was selected. The red line and the pink line in Fig. 11 show the Kalman filtering results. Compared to the concentration of CO_2 in spring, the winter concentration was higher due to the increased fossil fuel combustion caused by winter heating and weakening of plant photosynthesis. We select the smallest changes of CO_2 and H_2O concentrations around 5h for comparison of measurement precision between 1s raw data and the Kalman filter. The standard deviations of CO_2 and water vapor measurement data in the blue box of Fig. 10 were calculated and shown in Fig. 11. The 1 second raw measured concentrations yielded a 1 σ precision of 26.54 ppmv for CO_2 and 0.058% for water vapor, respectively. The

measurement precision of CO_2 and water vapor of the Kalman filter results were 9.22 ppmv and 0.027 %, improved by almost 2.9 times for CO_2 and 2.1 times for water vapor respectively. The Kalman filtering technique can efficiently reduce the shot-to-shot real-time noise and improve the measurement precision without affecting the time resolution and can improve the quality of the system real-time measurement results.

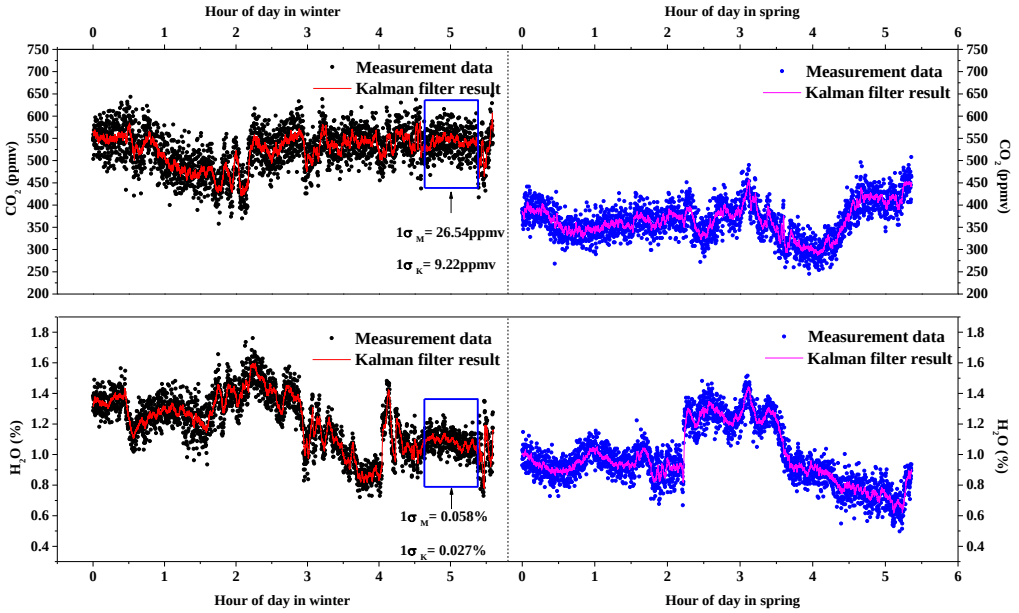

Fig. 11 Time series of atmospheric CO_2 and water vapor in two days in winter and spring with 1s measurement data and Kalman filter results. The standard deviations of CO_2 and water vapor measurement data in the blue box were shown. The measurement precision of the Kalman filter results were improved by almost 2.9 times and 2.1 times than those in 1s measurement data for CO_2 and water vapor respectively.

V. Conclusion

In this paper, an ultra-stable and high sensitivity HWG gas sensor is reported for the simultaneous measurements of CO_2 and water vapor in ambient air by a comprehensive study and optimization of different parameters in the system. The laser wavelength modulation parameters and gas pressure in the HWG were optimized to improve the strength of the WMS-2f signal, and hence the detection limit, where 14.5-time for CO_2 and 8.5-time for water vapor improvement in system detection limit were achieved compared to that working at atmospheric pressure. The influence of different parameters, including light coupling style and the scanning frequency of the laser were investigated. Our study showed that light coupling plays an important role to the stability of the HWG based sensor system. The scanning frequency is also found to affect the stability of the HWG sensor. After parameter optimization, the developed HWG gas sensor achieves a relatively good performance in terms of stability time (160s) and sensitivity (3 ppmv for CO_2 and 0.018 % for water vapor), which is important for real-time atmospheric gas detection. Ambient CO_2 and water vapor has been simultaneously measured by the developed HWG gas sensor for two days in winter and spring separately. A measurement precision with an average time of 1s by applying a Kalman adaptive filter obtains a 2.9-time improvement for CO_2 and 2.1-time improvement for water vapor compared to raw measurements. In summary, this work demonstrates the ability of HWG gas sensor for environmental monitoring and potential to be used in other areas, such as industrial production and biomedical diagnostics.

References

[1] J. E. Hansen, M. Sato, A. Lacis, R. Ruedy, I. Tegen and E. Matthews, "Climate forcings in the industrial era," *Proc. Nat. Acad. Sci*., vol. 95, no. 22, pp. 12753-12758, Oct. 1998.

[2] T. F. Keenan, D. Y. Hollinger, G. Bohrer, D. Dragoni, J. W. Munger, H. P. Schmid, A. D. Richardson, "Increase in forest water-use efficiency as atmospheric carbon dioxide concentrations rise," *Nature*, vol. 499, pp. 324-327, Jul. 2013.

[3] B. E. Law, E. Falge, L. Gu, D. D. Baldocchi, P. Bakwin, P. Berbigier, K. Davis, A. J. Dolman, M. Falk, J. D. Fuentes, A. Goldstein, A. Granier, A. Grelle, D. Hollinger, I. A. Janssens, P. Jarvis, N. O. Jensen, G. Katul, Y. Mahli, G. Matteucci, T. Meyers, R. Monson, W. Munger, W. Oechel, R. Olson, K. Pilegaard, K. T. Paw U, H. Thorgeirsson, R. Valentini, S. Verma, T. Vesala, K. Wilson, S. Wofsy, "Environmental controls over carbon dioxide and water vapor exchange of terrestrial vegetation". *Agr. Forest Meteorol*., vol. 113, no. 1-4, pp. 97-120, Dec. 2002.

[4] M. W. Sigrist, R. Bartlome, D. Marinov, J. M. Rey, D. E. Vogler, H. Wächter, "Trace gas monitoring with infrared laser-based detection schemes". *Appl.Phys. B*, vol. 90, pp. 289-300, Feb. 2008.

[5] J. U. White, "Long optical paths of large aperture". *J.Opt.Soc.Am*., vol. 32, pp. 285-288, May 1942.

[6] D. Herriott, H. Kogelnik, and R. Kompfner, "Off-axis paths in spherical mirror interferometers. *App.Opt*., vol. 3, pp. 523-526, Apr. 1964.

[7] E. R. Crosson, "A cavity ring-down analyzer for measuring atmospheric levels of methane, carbon dioxide, and water vapor," *Appl.Phys. B*, vol. 92, pp. 403-408, Aug. 2008.

[8] C. Li, L. Dong, C. Zheng, F. K. Tittel, "Compact TDLAS based optical sensor for ppb-level ethane detection by use of a 3.34 μm

room-temperature CW interband cascade laser," *Sensor. Actuat. B-Chem.*, vol. 232, pp. 188-194, Sep. 2016.
[9] E. Garmire, T. McMahon, and M. Bass, "Propagation of infrared light in flexible hollow waveguides," *Appl. Opt.*, vol. 15, no. 1, pp. 145-150, Jan. 1976.
[10] J. Li, Z. Du, Z. Zhang, L. Song, Q. Guo, "Hollow wave-guide-enhanced mid-infrared sensor for fast and sensitive ethylene detection," Sensor Rev., vol. 37, no. 1, pp. 82-87, Jan. 2017.
[11] Z. Wang, Y. Zhuang, A. Deev, S. Wu, "MIR hollow wave-guide (HWG) isotope ratio analyzer for environmental applications," in *Proc. SPIE* 10210, 2017, 1021009.
[12] W. A. Challener, M. A. Kasten, J. Karp, N. Choudhury, "Hollow-core fiber sensing technique for pipeline leak detection," in *Proc. SPIE* 10539, 2018, 105390P.
[13] S. Wang, Z. Du, L.Yuan, Y. Ma, X. Wang, R. Han, and S. Meng, "Measurement of Atmospheric Dimethyl Sulfide with a Distributed Feedback Interband Cascade Laser," *Sensors*, vol. 18, no. 10, pp. 3216, Sep. 2018.
[14] Z. Du, J. Wan, J. Li, G. Luo, H. Gao, and Y. Ma, "Detection of atmospheric methyl mercaptan using wavelength modulation spectroscopy with multicomponent spectral fitting," *Sensors*, vol. 17, no. 2, pp. 379, Feb. 2017.
[15] L. Liu, B. Xiong, Y. Yan, J. Li, Z. Du, "Hollow waveguide-enhanced mid-infrared sensor for real-time exhaled methane detection," *IEEE Photonic. Tech. L.*, vol. 28, no. 15, pp. 1613-1616, Apr. 2016.
[16] B. Xiong, Z. Du, L. Liu, Z. Zhang, J. Li, and Q. Cai, "Hollow-waveguide-based carbon dioxide sensor for capnography," *Chin. Opt. Lett.*, vol. 13, no. 11, pp. 111201, Sep. 2015.
[17] Z. Du, W. Zhen, Z. Zhang, J. Li, N. Gao, "Detection of methyl mercaptan with a 3393-nm distributed feedback interband cascade laser," *Appl.Phys. B*, vol. 122, pp.100, Apr. 2016.
[18] Y. Matsuura, T. Abel, and J. A. Harrington, "Optical properties of small-bore hollow glass waveguides," *Appl. Opt.*, vol. 34, no. 30, pp. 6842-6847, Oct. 1995.
[19] K. Matsuura, Y. Matsuura, J. A. Harrington, "Evaluation of gold, silver, and dielectric-coated hollow glass waveguides," *Opt. Eng.*, vol. 35, pp. 3418-3422, Dec. 1996.
[20] D. Francis, J. Hodgkinson, B. Livingstone, P. Black, and R. P. Tatam, "Low-volume, fast response-time hollow silica waveguide gas cells for mid-IR spectroscopy". *Appl.Opt.*, vol. 55, pp. 6797-6806, Sep. 2016.
[21] G. J. Fetzer, A. S. Pittner, P. E. Silkoff, "Mid-infrared laser absorption spectroscopy in coiled hollow optical waveguides," in *Proc. SPIE*, 4957, 2003, 124.
[22] J. Chen, A. Hangauer, R. Strzoda, M. Fleischer, and M. Amann, "Low-level and ultralow-volume hollow waveguide based carbon monoxide sensor" *Opt. Lett.*, vol. 35, no. 21, pp. 3577-3579, Oct. 2010.
[23] HITRAN on the Web. Available online: http://hitran.iao.ru/molecule.
[24] T. Zhou, T. Wu, H. Zhang, Q. Wu, W. Chen, C. Ye, and X. He, "Influence of light coupling configuration and alignment on the stability of HWG-based gas sensor system for real-time detection of exhaled carbon dioxide". *IEEE SENS. J.*, vol. 19, no. 24, pp. 11972-11979, Dec. 2019.
[25] P. Werle, R. Mücke, F. Slemr, "The limits of signal averaging in atmospheric trace-gas monitoring by tunable diode-laser absorption spectroscopy (TDLAS)," *Appl.Phys. B*, vol. 57, pp. 131-139, Aug. 1993.
[26] T. Wu, W. Chen, E. Kerstel, E. Fertein, X. Gao, J. Koeth, K. Röβner and D. Brückner, "Kalman filtering real-time measurements of H2O isotopologue ratios by laser absorption spectroscopy at 2.73 μm". *Opt.Lett.*, vol. 35, no. 5, pp. 634-636, Feb. 2010.
[27] B. Fang, W. Zhao, X. Xu, J. Zhou, X. Ma, S. Wang, W. Zhang, D. S. Venables and W. Chen, "Portable broadband cavity-enhanced spectrometer utilizing Kalman filtering: application to real-time, in situ monitoring of glyoxal and nitrogen dioxide," *Opt. Express*, vol. 25, no. 22, pp. 26910-26922, Oct. 2017.

Tao Wu received his PH.D. degree in Optics from University of the Littoral Opal Coast and Anhui Institute of Optics and Fine Mechanics, China. In 2010, Dr. Wu joined Key Laboratory of Nondestructive Test (Ministry of Education) of Nanchang Hangkong University, China. His main research interest has been the development of high-sensitivity laser spectrometer for laboratory and field studies of atmospheric trace gases and aerosols.

Weiping Kong received the B.E. degree from East China University of Technology in 2016. Since 2016, he has been a Graduate Student with the School of Measuring and Optical Engineering, Nanchang Hangkong University. His research interests include optical fiber sensing and gas absorption spectrum.

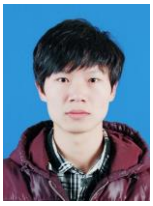

Mengyu Wang received Bachelor degree in Harbin Institute of Technology in 2015. He is currently pursuing his PhD in instrument science and technology in University of Science and Technology of China. In 2019, Mr. Wang joined Key Laboratory of Nondestructive Test (Ministry of Education) of Nanchang Hangkong University, China. His research interests include optical resonator, fiber optics, crystal optics, optical sensors and laser spectrum.

Qiang Wu received the B.S. and Ph.D. degrees from Beijing Normal University and Beijing University of Posts and Telecommunications, Beijing, China, in 1996 and 2004, respectively.,From 2004 to 2006, he worked as a Senior Research Associate in City University of Hong Kong. From 2006 to 2008, he took up a research associate post in Heriot-Watt University, Edinburgh, U.K. From 2008 to 2014, he worked as a Stokes Lecturer at Photonics Research Centre, Dublin Institute of Technology, Ireland. He is currently an Associate Professor at Northumbria University, U.K. His research interests include photonics devices and fiber optic sensing.

Weidong Chen received his B.S. (1992) from Zhongshan University, M.S. (1998) and Ph.D. degree (1991) from the University of Science and Technologies of Lille in France. He is full professor of physics at the University of the Littoral Opal Coast, Dunkerque, France. His current research interests include: development of photonic instrumentation for applied spectroscopy, optical metrology (concentration, isotope ratio) of trace gases for applications in atmospheric photochemistry and environmental science, and optical parametric laser source generation by frequency conversion and its applications to applied spectroscopy.

Chenwen Ye is a lecturer at the School of Measuring and Optical Engineering, Nanchang Hangkong University.

Rongjing Hu is working at Nanchang Hangkong University

Xingdao He was born in Jingan, China, in 1963. He received the Ph.D. degree in optics from Beijing Normal University, Beijing, China, in 2005. He is currently a Professor with the Key Laboratory of Nondestructive Test (Ministry of Education), Nanchang Hangkong University, China. His current research interests include light scattering spectroscopy, optical holography, and information processing.